International Journal of Modern Engineering Research (IJMER)
www.ijmer.com Vol.3, Issue.2, March-April. 2013 pp-928-938 ISSN: 2249-6645

Effect of Fuel and Air Injection Pattern on Combustion Dynamics in Confined and Free Diffusion Flame

M. A. Abdel-Al, [1] M. A. Yehia, [2] M. R. Taha, [3] T. W. Abou-Arab[4]
[1]*Mechanical Power Engineering, Faculty of Engineering, Cairo University, Egypt*
[234]*Prof. of Mechanical Power Engineering, Faculty of Engineering, Cairo University, Egypt*

Abstract: *A new burner is developed and its performance is experimentally studied. The principle of this new burner, circumferential alternative air and fuel burner (CAFB) is to admit fuel and air circumferentially alternative patterns. This burner also allow for swirling both fuel and air jets injecting from different circumferential holes. The outlet angle of air and fuel jet is changed between 0, 15, 30, 45 and 60 injection angles. A new definition and number for swirl is defined, this is called the Injection Swirl Number (ISN) and found to be accurate to describe the flame characteristics.*

Complete test rig was developed to facilitate characterization of the new burner. A new micro controller traverse mechanism was programmed and fabricated to control the sensitively moving of the thermocouple and gas analyzer sampling probe in all directions. Measurements of gas temperature at different positions, and the oxygen concentrations at the flame centerline were made. The thermal and chemical flame heights were obtained from the maximum temperature and oxygen concentration at the flame centerline. The visible flame height was obtained from direct photography and Infrared (IR) radiometry. The vortex breakdown creation period as a results of a high intensity swirling flow were been captured by the infrared radiation camera.

Comparisons of the new CAFB with other flames have also been performed. Experiments showed that the flame height decreases with the increase of the injection jet angles which improves the mixing between air and fuel generating an intense combustion zone and, hence, shortens the flame length. A new injection swirl ratio has been introduced for the new CAFB burner namely the injection swirl number (ISN), ISN = tan θ, where θ is the injection angle. The injection swirl number (ISN) used is 0, 0.26, 0.58, 1 and 1.75 which corresponding to the injection angles 0, 15, 30, 45 and 60 degree respectively. An empirical correlation has been derived for the new CAFB burner flame length as a function of the new derived (ISN).

Keywords: *Burner–Swirl–confined/free diffusion flame–flame length–Combustion efficiency–Injection angle*

I. Introduction

Combustion is the oldest technology of mankind and has furnished man with a major source of energy for more than one million years and at present, about 90% of our worldwide energy support (e.g., in traffic, electrical power generation, heating) is provided by combustion.

Multiple co- or counter- rotating swirlers with distributed fuel injection system characterize modern gas turbine combustion systems. Swirling flows are commonly used to improve and control the mixing process between fuel and oxidant streams to achieve flame stabilization and enhance heat release rate. The organization of swirling flow field governs the main flow structure; its match-up with fuel distribution is the key for achieving homogeneity of fuel/air mixture and consequently low NOx emission.

The most commonly used parameter for characterizing swirling flows is the swirl number SN, which is defined as the ratio of axial flux of the angular momentum Gφ to the axial momentum Gx [1]

$$S_N = \frac{G_\varphi}{G_x R} \qquad \textbf{(1-1)}$$

$$G_\varphi = \int_0^R (Wr)\rho U 2\pi r dr \qquad \textbf{(1-2)}$$

$$G_x = \int_0^R U\rho U 2\pi r dr \qquad \textbf{(1-3)}$$

Where U, W are the axial and tangential components of the velocity; R is the radius of the cross section plane; r is the radial coordinate. This swirl number characterizes the strength of swirling flow. It is commonly agreed that a vortex breakdown will occur in swirling flow if the swirl number exceeds certain limit, e.g. 0.6 for swirling flow without expansion cone.

Combustion will affect the shape of recirculation zone and the turbulence intensity of swirling flow. Experimental results based on pitot tube [1] showed that combustion induce comparatively small changes in aerodynamics of swirling flow fields; the boundary of recirculation zone and reversed mass flow rate are only slightly reduced compared with isothermal

cases. LDV measurement for swirling flow of reacting and nonreacting cases revealed that: compared with the isothermal case, the turbulence kinetic energy and velocity fluctuation substantially increased due to combustion, and the axial velocity increased for the combustion case because of gas expansion caused by heat release.

Rotating direction of each swirler component in multiple swirler configurations have significant effects on flow structures, temperature fields and exhaust gas concentrations. Due to the complexity of this problem, experimental results show different aspects of the physics and people made controversial observations. Counter-rotating swirl generated a large recirculation zone and large turbulent velocity fluctuation in the inter region of jet shear layer, consequently with observation of low oxides of nitrogen (NOx), high carbon monoxide (CO), and lower temperature field [2]. Recently, experimental data show that a consequence of the counter-rotating swirl brings up larger area of near-stoichiometric mixture of fuel and air, resulting in higher temperature field distribution within the stabilization zone compared with the co-rotating swirl case. To clarify the influence of rotating direction of swirl on combustion, it is necessary to correlate information of flow structures to combustion dynamics and emissions based on state-of-art laser diagnostics, optical sensing technology and emission analyzer.

Makel and Kenndy [3] measured the carbon atoms concentrations in diffusion of Sidebotham and Glassman [4]. Takagi et al [5], have carried out their investigation on two types of double concentric jet burner nozzles with different air and fuel locations, as one with the central air surrounded by fuel stream and the second is the opposite.

Wentzell [6] investigated new pattern for fuel and air admission. This pattern consisting of a central air jet surrounded by fuel stream in unconfined condition. He measured the flame temperature and flame length at different fuel and air jet diameters and at different fuel and air Reynolds numbers. Lee et al [16] applied an ethylene central air diffusion flame for the synthesis of carbon nano-tubes on a catalytic metal substrate. In a trial to investigate the effect of burner geometry on flame shape.

As a combination of premixed and diffusion flames, circumferential alternative air and fuel burner CAFB is capable of exploiting the advantages of both premixed flames and diffusion flames, in regards to operational safety, pollutant emission, and flame stability. Specifically, circumferential alternative air and fuel burner CAFB have no flash-back, a wide range of operational conditions and flexibility in flame length adjustment, coupled with potential NOx-reburning capability. These advantages of circumferential alternative air and fuel burner CAFB and their potential industrial and domestic applications have motivated this research work.

In this paper, a new burner is developed and its performance is experimentally studied. The principle of this new burner CAFB is to admit fuel and air circumferentially alternative patterns. This burner also allow for swirling both fuel and air jets injecting from different circumferential holes. The outlet angle of air and fuel jet is changed between 0, 15, 30, 45 and 60 injection angles. A new definition and number for swirl is defined, this is called the Injection Swirl Number (ISN) and found to be accurate to describe the flame characteristics.

II. Experimental Setup

The test rig shown in figure (1) consists of a main burner, oxidizer supply system, fuel supply system, flow controllers and measuring devices which hold in the Cairo university laboratory. The burner under investigation was fixed on a vertical position and a new transverse mechanism could be moved in the x, y, and z- directions. A new software programming is designed to move in a step control using the micro control technique to ensuring the high accuracy measurements. The traversing mechanism which carries thermocouple and gas sampling probe, supports by PIC microcontroller chips16F877 type as shown in figure (4.2). It offers all microcontroller I/O pins to external connectors for direct port accessing , while provides the most common primary devices and circuits , such as 2 X 16 LCD, Multiplexed 7SEG, Matrix KEYPAD, variable analog voltage, and RS232 serial interface. Thus, it saves most of the wasted time and efforts in hardware design and test,

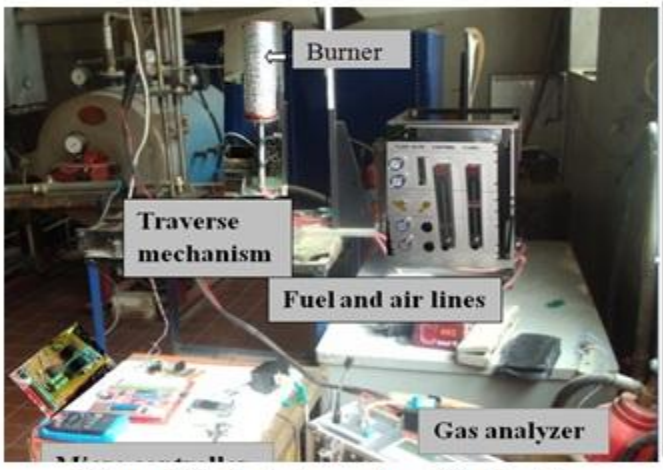

Figure (1): A photograph of the test rig

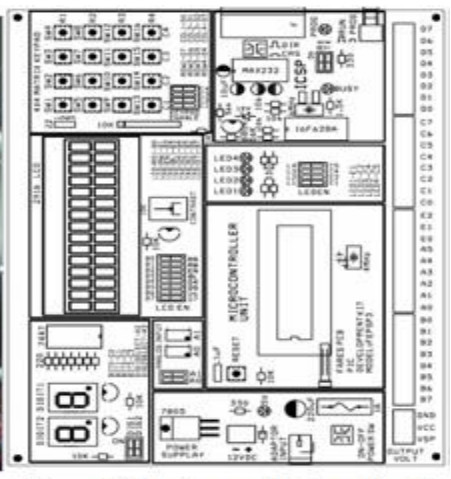

Figure (2): microcontroller circuit diagram

2.1 Air and fuel supply

The fuel used in this work is a bottled liquefied petroleum gas LPG (50% Propane, 50% Butane). A pressure regulator is mounted directly at the exit of the gas bottle to control the exit pressure of the fuel. The supplying of fuel is controlled by two needle valves which used to switch the fuel line between two rotameters (Dwyer Instruments Inc) with different ranges,

The primary air is supplied continuously from a reciprocating compressor equipped with a large storage tank (2 m^3) and delivers a pressurized air up to 10 bars. The air is regulated and delivered to the rotameter (Dwyer Instruments Inc). Pressure gauges are used to measure the pressure of the air and fuel before delivering to the test section, the flow-rate readings taken were corrected according to the calibration equations supplied by the manufacturer for the flow pressure.

2.2 Burner

Establishing the circumferentially alternated ports burner, (CAAB) diffusion flame, requires separate fuel/air supply systems enabling alternative distribute and supply of oxygen and fuel through burner holes. The reacting system is composed of three parts, namely, the burner tube, burner disc and the combustion chamber (combustor). The air and fuel jets are annular alternated to each others at the circumferential of the circular burner disc with sixteen equally distributed ports, each of 2.4 mm in diameter. The sixteen (eight to the each) ports are arranged alternatively in a circular array with an angular distance of 22.5º and the central distance is 11.5 mm to the head center line. The thickness of the burner head is 5 mm. The even air jets are directly connected to the air supply which passes through the burner tube. The odd fuel jets accumulate in the fuel chamber to equalize the flow from the fuel supply by placing layers of grids in the chamber. The grid layers are to ensure that the flow from each of the fuel and air ports is equal as shown in Figure (3).

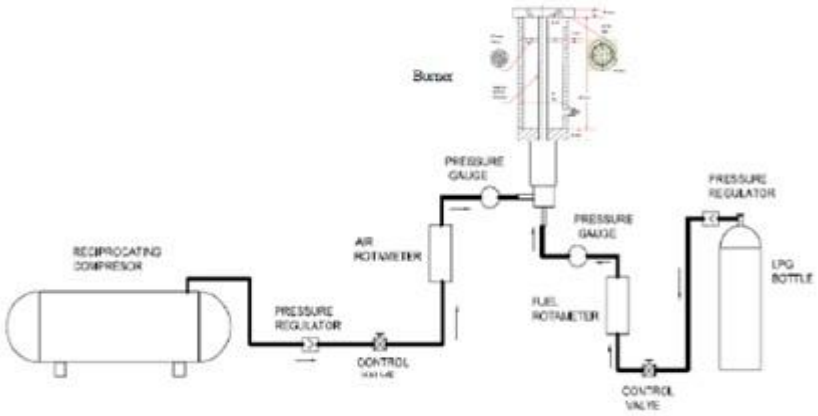

Figure (3): Flow diagram of the fuel and oxidizer

The main reason of the improvement of fuel/air interaction is in the smart design in the CAFB burner nozzle, in which each fuel stream is embedded between two air streams, and vice versa such that each air stream is localized between two main fuel streams, and finally the two air and fuel streams are rotated with each others. It means a higher volume to surface ratio for the fuel and the oxidizer, which increases the shear layers acting as a rapid mixing mechanism. The burner outwards flow rotates in a tangential injection bore angles. For parametric study and optimization, these angles varied to covering the entire available tangential span. The burner holes injection angles exhibits at 0, 15, 30, 45 and 60 degree Stability occurs mainly due to the IRZ by the recirculation flow process. A schematic of the design of the CAFB diffusion flame burner is shown in figure (4).

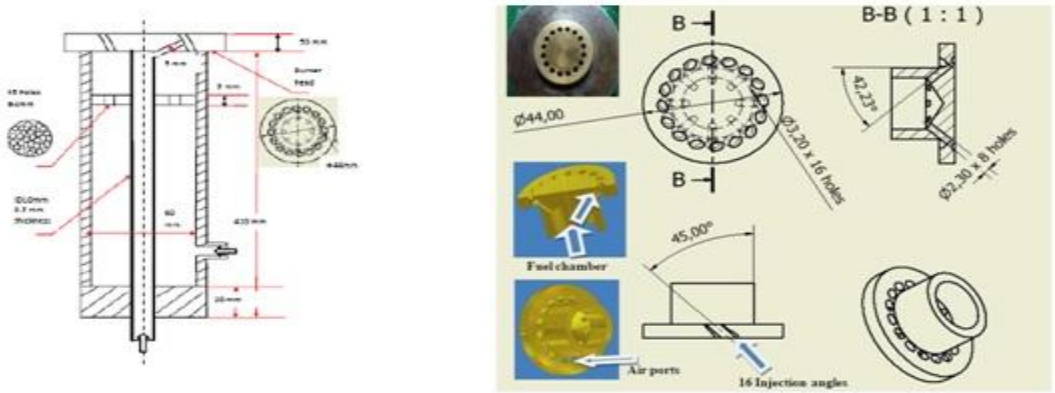

Figure (4) Schematic of the circumferentially alternated ports (CAAB) burner

2.3 Combustor

The combustor as shown in Figure 5 is an iron cylinder with 300mm diameter and 600mm length; there are 60 holes along the surface of confinement at successive distance of 5mm in the axial direction. These holes are used for inserting thermocouple or gas analyzer probe. A rectangular sight glass (200mm x 500mm) is mounted on the outer surface of the confinement and sealed to prevent leakage; this sight glass is used to facilitate capturing photos for flames. The exhaust section was ended by a cone with 40mm exit diameter to eliminate air entrainment.

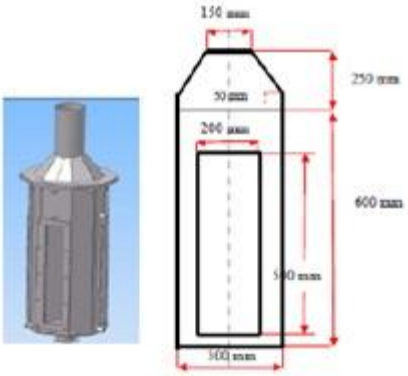

Figure (5): Schematic of the combustor

2.4 Measuring Techniques

A Nikon COOLPIX 990 digital camera is used to take the flame photographs. The camera has 3.1 million effective pixels. The major adjustable parameters of the camera are the exposure time and the aperture stop. In this study, an aperture of 3.6 is used for each photograph. The exposure time used for these photographs is 1/4th of a second to obtain global information on the average flame image. In this investigation the camera is mounted on a tripod (model Manfrotto 3021PRO) to ensure stable camera positioning. The height of the tripod was fixed at 125 cm from the floor of the lab. The distance from the test section was set with the legs fully spread and the front leg touching the base of the burner stand. The distance between the camera and the fuel nozzle exit is approximately 75 cm. The lens is positioned in line with the top of the burner exit plane injector. Black painted aluminum sheets are placed behind the flame and on top of the test section bottom plate. This is done to eliminate reflections of the flame in the photographic image.

A thermal imager used is a ThermaCAM SC 3000 & TI45 with cooled quantum well infrared photodetector (QWIP) manufactured by FLIR. The detector is 320 x 240 pixels that detect an infrared signal in the 8-9 micrometer range. It is stirling cooled down to 70K and has a cooling down time of less than 6 minutes. The basic operation of the camera is to detect the electromagnetic energy radiated in the IR spectral band from the flames. It then converts the radiated energy into an electronic video signal. The IR energy is first radiated through a medium (typically the atmosphere). It then enters the sensing system, passing through a lens, a filter, and finally incidents on a single IR detector or a focal plane array (FPA) sensor, which transforms the radiation into an electrical signal. The radiance captured by an infrared camera depends mainly on the object temperature, background temperature and emissivity of the source object.

The temperature is measured by a bare wire thermocouple. The measuring temperature has been corrected to eliminate the effect of radiation and conduction errors initiated when measuring the temperature by the bare wire thermocouple inside the flame. The type of thermocouple used is a type-B thermocouple (Platinum-6% Rhodium vs. Platinum-30% Rhodium) with a diameter of 200 μm, and length of 20 cm, manufactured by OMEGA Engineering Inc., the wire of the thermocouple is inserted in a fine ceramic tube of 1.5 mm diameter to insulate them.

The data acquisition system used consists of a data acquisition card (type NI6024M series, maximum sampling rate 200 kHz, ± 10 v input). The data acquisition card was installed in a personal computer and programmed via Labview. The program function is to record the differential voltage coming from the thermocouple with a rate of 500 Hz/s and a sampling time of 20 s, then calculate the mean of every 10 sample before calculating the total mean of reading to illuminate the effect of fluctuation and noise generating due to measurements. An I/O Connector Block with 4 Signal Conditioning slots for use in integrating thermocouple is used between the connection of thermocouple and data acquisition card to isolate voltage input into the measurement system. The type of I/O Connector Block is SCC-68 which is also a product of national instrument company.

The emission concentrations were measured using IMR-2800A gas analyzer. Gas samples are withdrawn from the flame by a water-cooled sampling probe. Three concentric stainless steel tubes of 1.5 mm and 4 mm and 6 mm outside diameter with length of 20 cm are used as a cooled probe.

III. Results and Discussions

3.1 Flame stability & different burner designs

The burner introduces the flow pattern into the combustion chamber with the recirculation induced flow by collection of the two ways of stabilization mechanisms namely swirl and bluff body nozzle concepts. The burner outwards flow rotates in a tangential injection bore angles. For parametric study and optimization, these angles varied to covering the

entire available tangential span. The burner holes injection angles exhibits at 0, 15, 30, 45 and 60 degree. The corresponding swirl number is 0, 0.3, 0.6,1 and 1.75 respectively. A comparative study with the traditional designated swirlers is utilized in this study. The new burner is a circumferential air and fuel burner denoted as (CAFB), in which the eight fuel ports are alternatively circumferentially arranged with the eight air ports. Stability occurs mainly due to the IRZ by the recirculation flow process. The IRZ, being storage of heat and chain carriers, carries heat and active chemical species towards the root of the flame, and ignites the fresh mixture of fuel and air. Therefore, between the forward going reactants and the reverse flow of the combustion products is the flame front which is associated with intensive mixing and combustion.

Figure (6) shows a flame stability map of the new burner (CAFB) at different injection angles. The conclusion drawn from this Figure is that the optimum injection angle. Therefore the experimental work and parametric study are carried out at this optimum injection angle 30˚. The improved stability of this burner is due to the diffusion process, i.e. the fuel diffuses into the air and causes simultaneous mixing and combustion, thus the rate of combustion depends on the rate of mixing between the fuel and air rather than the much faster chemical reaction rate. Figure (6-a) also shows that the optimum injection angle is at 30 degree, in which the stability zone as increased and the extinction zone is decreased.

The optimum injection angle of 30˚exhibits in confined condition with a higher stability limits than the other injection angles as shown in Figure (6-b).

It is noticed that the stability limit increases as the injection angle increase up to 30o injection angle (ISN =0.6). At higher injection swirl number (ISN), an abrupt change in the structure of the core of a swirling flow which namely, vortex breakdown as a result of instability. This phenomenon agreed with the results and studies given in Escdier and Keller believing [18], and Syred Beer [19]. They proposed that when the flow reaches a certain swirl number, instability develops and the central forced region of flow starts to precess about the axis of symmetry. This precession forms the so-called precessing vortex core (PVC).

Using the infrared radiation technique for the flame visualization, we found that the incubation period for the precessing vortex core (PVC) based on the concept of the recirculation, core has a highly temperature zone at the flame basement. Therefore it can be seen microscopically in the infrared band width. Figure (7), shows the formation cycle of the PVC in free in Figure (7- a), and confined conditions in Figure (7 -b) respectively.

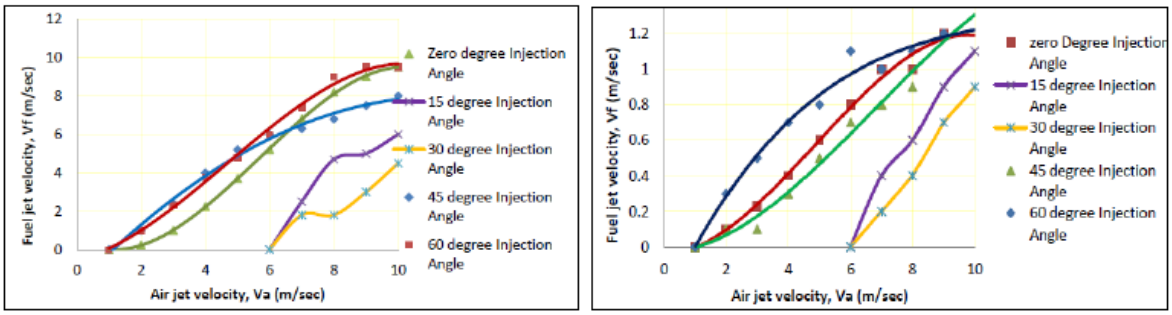

Figure (6): Flame stability limit at different injection swirl numbers (ISN),
(a) Free and (b) confined

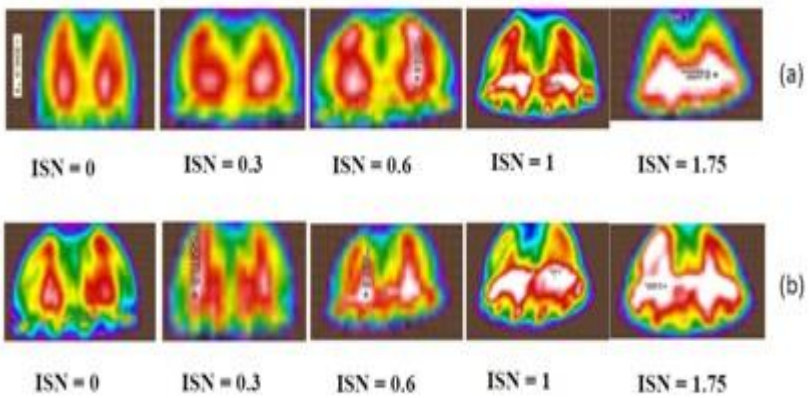

Figure (7): Formation cycle of PVC at different injection swirl numbers (ISN), (a) free and (b) confined conditions

It is shown clearly in the formation cycle mechanism that the PVC increases as the injection swirl number increase. When injection swirl number (ISN) exceeds 0.6, eddy shedding occurs as shown in Figure (7).

3.2 Combustion Efficiency

As basically known and as mentioned before, mixing improvement results in combustion efficiency increases due to the complete molecular diffusion level that speeds up between the fuel and oxidizer which enhances the combustion process. Combustion efficiency (ηc) is defined as:

(heat released in combustion)/(heat available in fuel)

$$\eta_c = 100\% - (m.g\ Cp_g(T_{exh.} - T_{amb}))/(m_f\ C_{pf}) \quad \textbf{(1-4)}$$

Where m_g……. the gas mass flow rate and equal to (mf + ma) from mass balance
T_{Exh}…. the average exhaust gas temperature at chimney accumulator
T_{amb}…...the ambient temperature (30˚C)
C_{pf}…….the lower calorific value of fuel

3.2.1 Effect of equivalence ratio on combustion efficiency

Figure (8) represents the effect of equivalence ratio on the combustion performance (efficiency). It shows that, when the equivalent ratio increases the combustion efficiency increase simultaneously, due to increasing of the fuel to air interaction in the new CAFB burner. Comparison between current experimental results and others shows an agreement and difference is attributed to same geometrical differences between current burner and others geometry for air and fuel admission.

The main reason of the improvement of fuel/air interaction is in the smart design in the CAFB burner nozzle, in which each fuel stream is embedded between two air streams, and vice versa such that each air stream is localized between two main fuel streams, and finally the two air and fuel streams are rotated with each others. It means a higher volume to surface ratio for the fuel and the oxidizer, which increases the shear layers acting as a rapid mixing mechanism.

Figure (8) shows higher combustion efficiency with the new CAAB burner as a result of complete combustion process due to the higher mixing efficiency as a result of increasing injection swirl number (ISN).

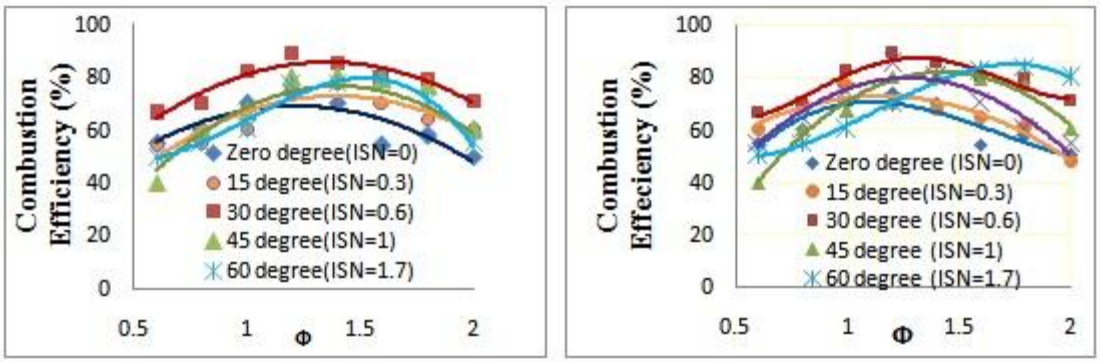

Figure (8): Combustion efficiency at different equivalence ratio and different (ISN),
(a) Free and (b) confined

3.2.2 Effect of ISN on combustion efficiency

The maximum combustion efficiency obtained at optimum injection swirl number (ISN) which corresponding to the burner stability curves was found to be about 90 % in the new burner (CAFB) compared to the others. For single swirled burner the combustion efficiency was (65%) Tomas et al [7], and for the circumferential fuel ports surrounding by a single central air jet (CAP) introduced by Sze [8] this combustion efficiency was (75%) in a free jet cases. In confined conditions as shown in Figure (9-b), the combustion efficiency reaches (85%) with the new CAFB burner and was the highest compared to four previous designs of burners of Brakely [9], Oymar Chiu [10], K.D. Kenshof [11] and Tomas et al [7] for the same heat release rates. The combustion efficiency in lower in confined than in free jets which may be due to the walls effects, and due to the entrainments effect in free jets.

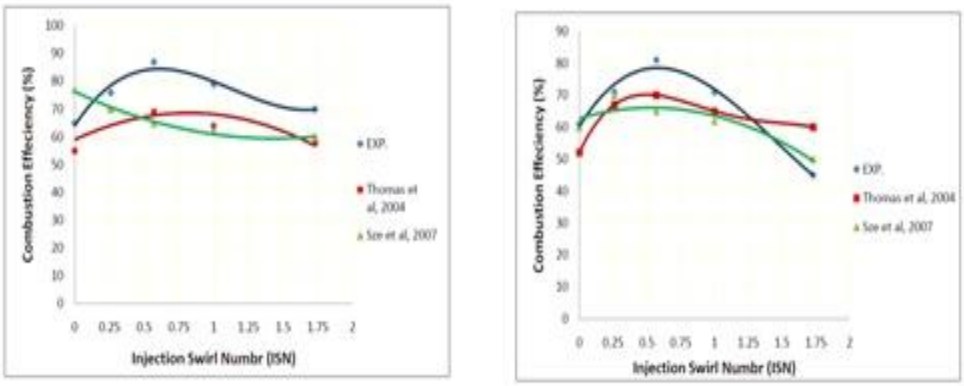

Figure (9): Effect of ISN on Combustion efficiency, ηc (%), (a) free and (b) confined

3.3 Flame Length

The visible flame length is an important parameter to determine the flame characteristics. As mentioned in the literature review, the flame length defines the high temperature zone for diffusion flame (temperature based flame length) and the global residence time available for pollutant formation within the flame (pollutant based flame length).
Generally in normal diffusion flame, combustion is controlled by diffusion of air molecule into the fuel stream. The effects of air flow rate and fuelling rate on flame length have been investigated in free and confined conditions, and the results are shown in the following sections. Photographic images of the average visual appearance of the new burner (CAFB) were obtained using a high resolution camera of 10 Mega pixels (CANON A 1000 SI). All Camera shots were taken in the night vision mode with shutter speed of 1/60 s to express the average flame shape. The visual flame length was measured by comparing the flame length in the photo by a reference length scale. For the real flame length evaluations, the thermal Infrared has been used to investigate the flame length which is related to the radiated photons from the flame in the infrared spectroscopy band.

3.3.1 Effect of air jet velocity and fuel jet velocity on flame length

Firstly, experiments were conducted to investigate the effects of air jet and fuel jet velocities on flame length. Fuel jet velocities of (1 to 10 m/sec) were used for the experiments while air jet velocities were varied from (1 to 10 m/sec). Secondly, experiments were carried out at a fixed air jet velocity of 6 m/sec while the fuel jet velocity was varied from 1 to 10 m/sec. The results are shown in Figure (10) in both free (a) and confined conditions (b). Figure (10) shows a decrease in the flame length when the air jet Reynolds number is increased from 2000 to 10000. It is observed that the flame is shorter in the new circumferential alternative fuel and air burner (CAFB) compared to the same air and fuel flow rates in single jet with central air and annular fuel jet in free diffusion flame studied by Valdiesh, [12] and F. D. Koalidof [13]. This is because of more intensive mixing with CAFB and hence more complete combustion occurs in the IRZ of the new burner. The flame length is longer in confined than in free flame at the same air and fuel flow rates and shorter than the non- swirled confined burner used by John K. et al [14] as shown clearly in Figure (10-b). Numerical simulation shows results nearly of same values of the experimental results in both of free and confined conditions.

The Reynolds number (Re) is increased progressively from zero to the maximum value for a stable flame to establish, and meanwhile the overall equivalence ratio (Φ) is kept at 1.5. This means increasing the volumetric flow rates of both fuel and air and simultaneously keeping their ratio unchanged. The resultant flame images are shown in Figure (10). To understand the effect of fuel flow rates on the flame length, the fuel jet velocities increased from 1 to 10 m/sec, while the air jet velocity remains constant at 6 m/s. basically, when the fuel jet velocity is increased, the fueling rate as well as the overall equivalence ratio is increased. Figure (11) shows an increase in the flame length when the fuel jet velocity is increased from 1 to 10 m/sec in both free (a) and confined condition (b). This is attributed to the increase of fuel jet momentum and therefore axial penetration in the flow field.

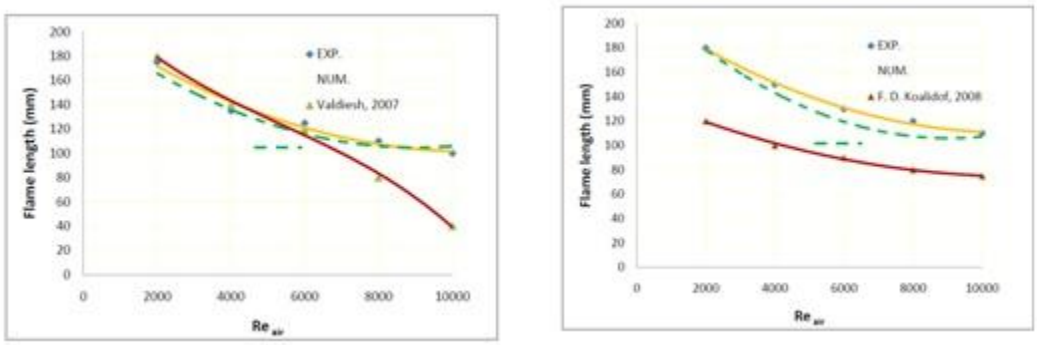

Figure (10): (a) Effect of Re on flame length, H (mm),(a) free (b) confined

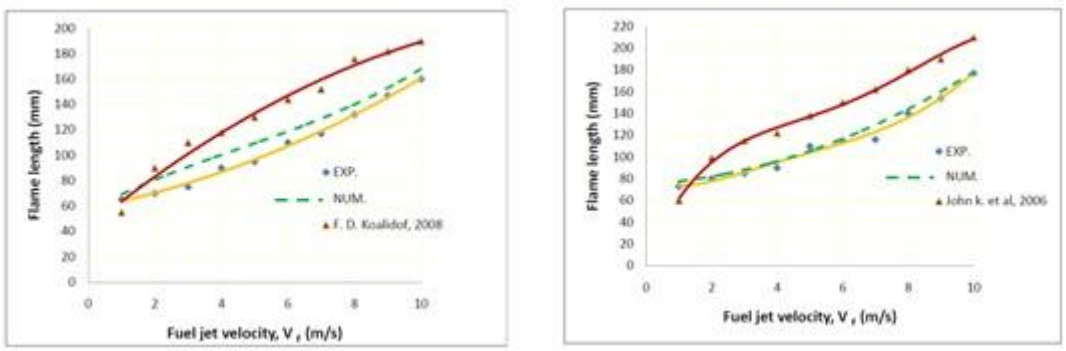

Figure (11): Effect of fuel jet velocity on flame length, H (mm), (a) free (b) confined

The camera or thermal imager used is a ThermaCam SC 3000, and TI 45 with cooled quantum well infrared photo detector (QWIP) manufactured by FLIR.

The infrared radiation comes from the flame has been observed by the ThermaCam shown in Figure (12), which presents the thermal flame length. The thermal flame length is agreed with the observed flame length from the digital camera, but the infrared image explains more details about the inner constructions of the flame length. An internal recirculation zone (IRZ) is formed in the centre of the flame, specifically in the centre of the flame root. The yellow color makes the IRZ easily recognizable to the naked eyes. The IRZ is observed to occupy a large proportion of the main flow field (flame root) due to a large portion of the initial flow being recirculated, and two vortexes reside symmetrically to the burner nozzle axis due to the rotational motion of the fluid. As the value of Re increases, the flame root augments in size and the flame tail diminishes in both size and length. Free condition in Figure (12) shows the long flame tail totally disappears and an entirely blue flame is formed, which is mainly premixed in nature because of more intensive mixing of the supplied fuel and air and hence more complete combustion. The blue colour makes the IRZ invisible to the eyes so that a flow visualization technique is of necessity for the purpose of visually observing the flame.

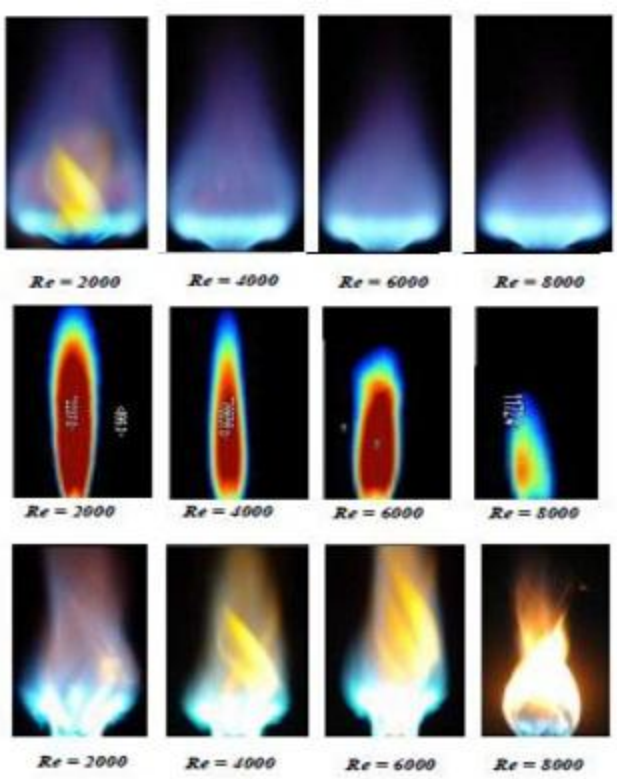

Figure (12): Flame images at different Re at fixed Φ = 1.5, free (upper), thermal and confined (lower) conditions

3.3.2. Effect of Air/Fuel ratio on flame length

Generally an increase in Φ corresponds to an increase in the amount of supplied fuel. The effect of equivalence ratio Φ on the flame length at fixed Re = 6000 is shown in Figure (13).

Figure (13) shows an increase in the flame length for both the swirling and the non-swirling flames, while the non-swirling flames are much longer than the swirling flames. The non-swirling flames are observed to consist of a premixed bluish flame overlapped by a diffusion flame, with a growth in the downstream diffusion flame as Φ increases from 1.0 to 2.0. However, the new burner CAFB remains fairly premixed in nature with the post-combustion zone, which is weakly diffusional in nature, becoming more and more observable with increasing Φ. A typical case at Re = 8000 with Φ increasing from 1.0 to 2.0 is shown in Figure(13). The increasing of equivalent ratio Φ means an increase in the amount of supplied fuel, thus the flame becomes more diffusional in nature and the flame length increases accordingly. It is clear from previous Figures that the flame length of the new burner CAFB is dependent on both Re and Φ, just as that in premixed flames Kwok et al. [15]. At fixed Re, for both swirling and non-swirling the CAFB burner lengthens the flame with increasing Φ due to increased fuel supply. Furthermore, the IRZ was found to play an important role in flame length shortening. The flame length variation with equivalence ratio is shown in Figure (13). The current experimental and numerical results are in partial agreement with the data of Sze et al 2007, but in full agreement with the trend.

As a result of the increasing amount of supplied fuel and due to the fact that Zone 3 or the post-combustion zone becomes more and more diffusional and thus as Φ increases from 1.0 to 2.0, the flame length increases monotonically.

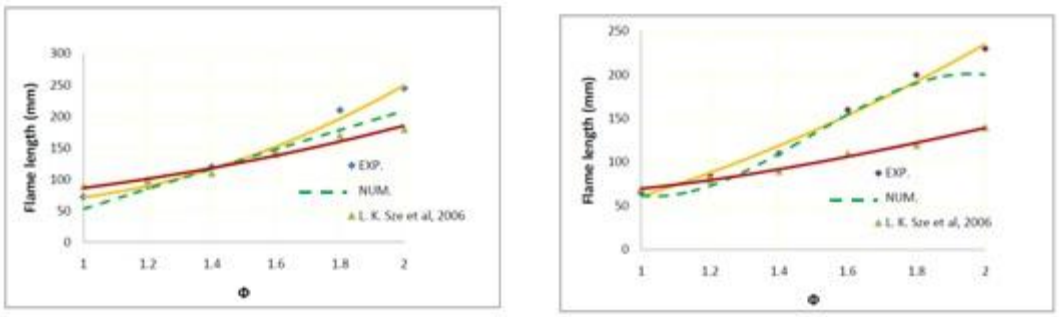

Figure (13): Effect of (Φ) on the flame length, (a) free (b) confined

3.3.3. Effect of Injection Swirl Number (ISN) on flame length

In theory, the IRZ is noticed when the actual swirl number is higher than 0.6. Below that, the weak adverse axial pressure gradient is not strong enough to induce a reverse flow. We found that, for the new circumferential air and fuel burner (CAFB), the flow injected at different injection angles of 0, 15, 30, 45 and 60 degrees rotated at different swirling intensities in so called a swirl number.

As mentioned in the literature review, there are several relations that can define the swirl number, however here we concluded a new number, namely, injection swirl number (ISN) which describes this circumferential air and fuel burner (CAFB).

The new formula accepted mathematically with the traditional Swirl Number formula.

The swirl number is defined by [1]:

$$S = \frac{G_{ang}}{R_b G'_x} = \frac{\int_0^{\infty} \rho U W r^2 dr}{R_b \int_0^{\infty} \rho (U^2 - \frac{1}{2} W^2) r dr} \qquad \textbf{(1-5)}$$

Where Gang is the angular momentum in the swirled section and G'x is the liniear momentum flux through the unswirled center core and the swirled annulus. This terms can be calculated by integrating the mean axial, U, and the mean swirl, W, velocity components across the burner exit. With the assumption that the distribution of the axial flow remains flat, and U and W at the burner exit are kinematically related to the blade angle as tan α = U/W , the axial flux of angular momentum in the annular section is then written as follows:

$$G_{ang} = 2\pi\rho \int_{R_c}^{R_b} U_a (U_a \tan\alpha) r^2 dr = 2\pi\rho U_a^2 \tan\alpha \left(\frac{R_b^3 - R_c^3}{3} \right) \qquad \textbf{(1-6)}$$

Here, Ua is a mean axial velocity supplied through the swirl annulus. By assuming flat axial velocity distribution, the linear momentum flux from the two regions of the burner is then calculated as follows:

$$G_x = 2\pi\rho \int_{R_c}^{R_b} U_a^2 r dr + 2\pi\rho \int_0^{R_c} U_c^2 r dr = \pi [\rho U_a^2 (R_b^2 - R_c^2) + \rho U_c^2 R_c^2] \qquad \textbf{(1-7)}$$

Where Uc is a mean axial velocity through the center core. With Equation (1) as defined, the geometric swirl number for the vane swirl burner is then:

$$S = \frac{\frac{2}{3}\tan\alpha(1 - R^3)}{1 - R^2 + \frac{U_c^2}{U_a^2} R^2} = \frac{2}{3}\tan\alpha \frac{1 - R^3}{1 - R^2 + [m^2 (1/R^2 - 1)^2] R^2} \qquad \textbf{(1-8)}$$

Where: α…..the injection angle

R….ratio of the center channel radius (Rc) to injector radius (Ri)

m….mass flux ratio (between mass flux through center channel (mc) and mass flux through swirl annulus (ms))

For the new burner (CAFB):

a- Channel radius is the injection radius (R≡1), let R=0.9 for simplicity.

b- Channel in annulus, so the center channel is the swirl annulus. i.e m=1.

Substitute in Equation (1-8) we got the new formula for the injection swirl number for the new burner (CAFB)..

S = 2/3 tanα (3/2)

i.e. **ISN = Tan □** **(1-9)**

Where θ is the injection angle tangent to the burner surface, and ISN is the new correlation for injection swirl number for the multi fuel jet in this case (CAFB).

Figure (14) show the effect of injection swirl number on the flame length, it shows that the flame length decreases as the injection swirl number increase. Figure (14) shows the flame length for CAFB burner is lower than the central air surrounded by the fuel ports described by Sander bad et al 2004 in free condition. In confined condition, the flame length decrease steeply as ISN increase. Figure (15-b) shows lower heights in CAFB burner with respect to the traditional burners compared to Sanderbad et al [33] in the similar confined conditions. On the other side and for further justifications and validation of present data, the numerical simulation gives a good agreement with the experimental results as shown in Figure (15-a and b)

It can be easily concluded that swirl greatly enhances the mixing of air and fuel streams causing the shorter flame length to both jet and swirl mixing parameters. A new semi-empirical correlation could be developed between flame lengths as a function of ISN.

$$\text{Flame length (mm)} = 58.69\,(\text{ISN})^3 + 72.00\,(\text{ISN})^2 - 543.9\,(\text{ISN}) + 467.4 \qquad \textbf{(1-10)}$$

The calculated flame length is consistent with the measured flame length in free jet only as shown in Figure (16). Figure (16) shows the flame height is about 0.51 m at ISN = 0, which is near to the result obtained photographically before. Figure (17) shows the flame height correlation in confined conditions with a dissatisfactory result with the experimental data. The main reason of the un-consistent in confined conditions is the flame disturbance due to the flame shedding and the flame wall interaction which disturb the flame where we cannot introduce an exact correlation.

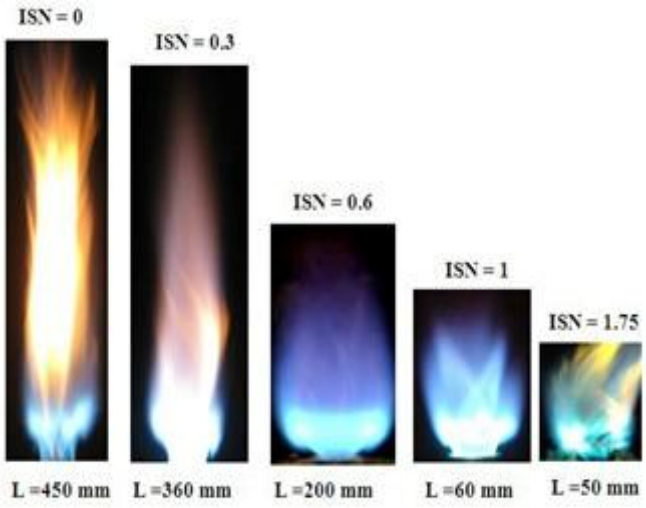

Figure (14): Photo images showing the effect of ISN on the flame

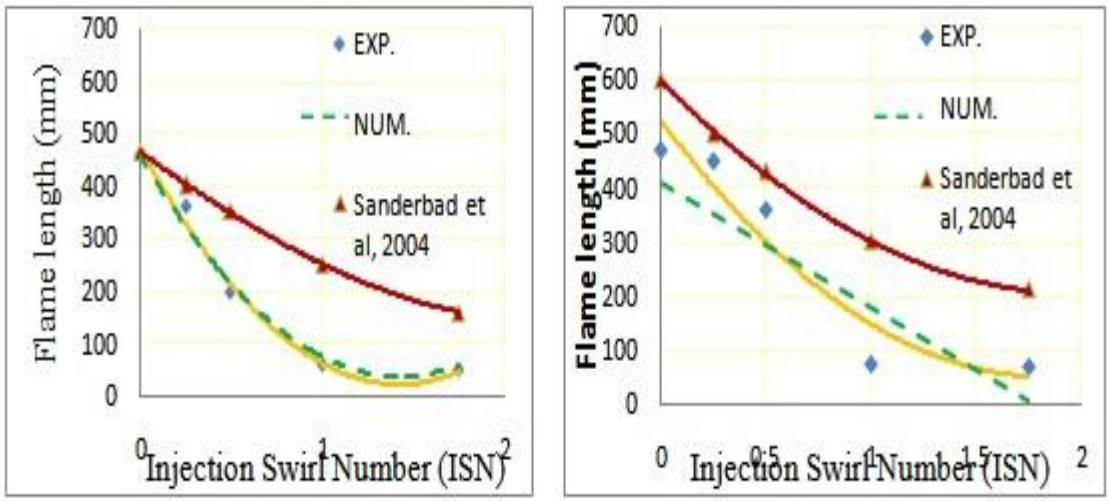

Figure (15): Effect of ISN on flame lengths, H (mm), (a) free (b) confined

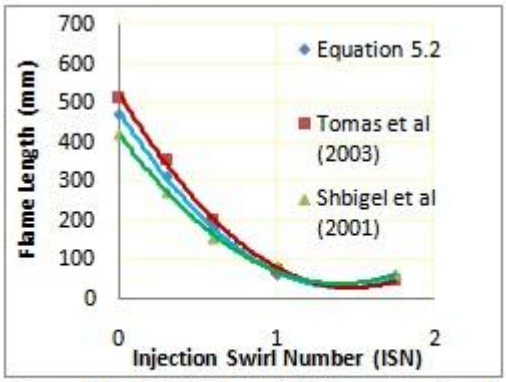

Figure (16a): Effect of ISN on correlated flame length (equation 1-10), free

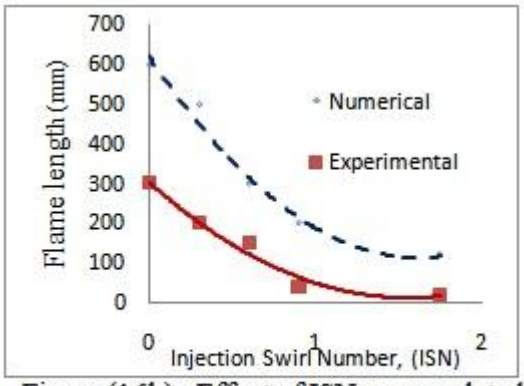

Figure (16b): Effect of ISN on correlated confined length (equation 1-10), confined

IV. Conclusions and recommendation

Experimental investigations have been conducted on the **characteristics** of the new burner including flame appearance, flame structure, flame temperature. Comparisons of the new CAFB with other flames have also been performed. The main conclusions can by summarized as:

- The optimum injection angle of 30˚exhibits in free/confined condition with a higher stability limits than the other injection angles.
- When the equivalent ratio increases the combustion efficiency increase simultaneously, due to increasing of the fuel to air interaction in the new CAFB burner. The maximum combustion efficiency obtained at optimum injection swirl number (ISN)which corresponding to the burner stability curves was found to be about 90 % in the new burner (CAFB) compared to the others
- The flame height decreases with the increase of the injection jet angles which improves the mixing between air and fuel generating an intense combustion zone and, hence, shortens the flame length.
- A new injection swirl ratio has been introduced for the new CAFB burner namely the injection swirl number (ISN), ISN = tan θ, where θ is the injection angle. The injection swirl number (ISN) used is 0, 0.26, 0.58, 1 and 1.75 which corresponding to the injection angles 0, 15, 30, 45 and 60 degree respectively.
- An empirical correlation has been derived for the new CAFB burner flame length as a function of the new derived (ISN).

References

[1] Beer, J.M, Chigier, N.A. Flame stabilization in recirculation zones of jets with swirl, Proceedings of the seventeenth International Symposium on Combustion, The Combustion Institute, 1971, 563.
[2] Syred, N. and Beer, J.M. Combustion in swirling flows: a review. Combustion and Flame, 1974, 23, 143-201.
[3] Makel, D.B. and Kennedy, I.M. Soot formation in laminar inverse diffusion flame. Combustion Science and Technology, 1993, 81, 207.
[4] Sidebotham, G..W. and Glassman, I. Flame temperature, fuel structure, and fuel concentration effects on soot formation in inverse diffusion flames. Combustion and Flame, 1992, 90, 269-283.
[5] Takagi, T., Xu, Z. and Komiyama, M. Preferential diffusion effects on the temperature in usual and inverse diffusion flames. Combustion and Flame, 1996, 106, 252-260.
[6] Wentzell J.C. The Characteristics and Structure of Inverse Flames of Natural Gas MSc Thesis, the Queen's University 1998.
[7] Tomas, G.B. and Jawurek, H.H. The ''hood method'' of measuring emissions of rural cooking devices. Biomass Bioenergy, 1999, 16, 341–345.
[8] Sze, L.K., Cheung, C.S. and Leung, C.W. Appearance, temperature and NOx emission of two inverse diffusion flames with different port design. Combustion and Flame, 2006, 144, 237-248.
[9] Brakely, S.P. and Schumann, T.E. Diffusion flames Industrial & Engineering Chemistry, 1988, 20, 988-1004.
[10] Oymer, B.L., Cziesla, T., Mitra, N.K. and Biswas, G. Numerical investigation of heat transfer in impinging axial and radial jets with superimposed swirl. International Journal of Heat and Mass Transfer, 1997, 40, 141-147.
[11] K. D. Ken Shaf and Gore, J.P. Flow structure in lean premixed swirling combustion. Proceedings of the Combustion Institute, 2002, 861-867.
[12] Valdiesh, L. Turbulent combustion modeling. Progress in Energy and Combustion Science, 2002, 28, 193-266.
[13] F. D. Koalidof. Experimental and Numerical Investigation of the Novel Low Nitrogen Oxide CGRI Burner PhD Thesis, the Queen's University, 1998
[14] John, k.G. The prediction of laminar jet diffusion flame size: Part I, Theoretical model. Combustion and Flame, 1977, 29, 219-226.
[15] Kwok, L.C., Leung, C.W. and Cheung, C.S. Heat transfer characteristics of an array of impinging pre-mixed slot flame jets. International Journal of Heat and Mass Transfer, 2005, 48, 1727-1738.